Available online at www.sciencedirect.com
SCIENCE DIRECT®
Marine Geology 204 (2004) 129–144
MARINE GEOLOGY
INTERNATIONAL JOURNAL OF MARINE GEOLOGY, GEOCHEMISTRY AND GEOPHYSICS
www.elsevier.com/locate/margeo

Glendonites and methane-derived Mg-calcites in the Sea of Okhotsk, Eastern Siberia: implications of a venting-related ikaite/glendonite formation

J. Greinert [a,*], A. Derkachev [b]

[a] GEOMAR Research Center for Marine Geosciences, Wischhofstrasse 1–3, D-24148 Kiel, Germany
[b] Pacific Oceanological Insitute, Far Eastern Branch of the Russian Academy of Sciences, POI, 43 Baltiyskaya Street, 690041 Vladivostok, Russia

Received 23 December 2002; received in revised form 19 September 2003; accepted 13 November 2003

Abstract

Mg-calcite-cemented bioturbation traces, glendonite aggregates of idiomorphic, bi-pyramidal crystals and porous, amber-colored carbonate concretions were recovered from a methane-dominated cold vent area in 380 m water depth at the northern Sakhalin Slope, Sea of Okhotsk. Bioturbation traces consist of Mg-calcite cemented sediment with $\delta^{13}C$ values between −37 and −46‰ PeeDee Belemnite (PDB), which implicate methane as the carbon source. Glendonite, a calcite pseudomorphosis after ikaite ($CaCO_3 \cdot 6H_2O$), and amber-colored concretions are both composed of varying amounts of calcite and Mg-calcite with $\delta^{13}C$ values between −19 and −34‰ PDB. Isotope analyses of an ikaite crystal recovered in the vicinity reveals $\delta^{13}C$ values between −20‰ and −22‰ PDB indicating organic matter as the carbon source. Microscopic investigations of glendonites and amber-colored concretions show a porous fabric of a primary calcite phase that is overgrown by a secondary Mg-calcite cement. As ikaite pseudomorphs to porous calcite and as carbon isotope values are the same for the ikaite and the high end member values of glendonite samples, the primary calcite phase is suggested to be a former ikaite phase. Because they share the equal color, fabric, mineral and isotopic composition with glendonites, the amber-colored concretions are also suggested to represent calcite that transformed from ikaite. A mixture of pseudomorph calcite ($\delta^{13}C$ −20‰ PDB), which originally formed as ikaite from degraded organic matter, and Mg-calcite ($\delta^{13}C$ −43‰ PDB), which crystallized due to the anaerobic oxidation of methane, can explain the varying carbon isotope data of the glendonites and the amber-colored concretions. The growth of ikaite, the transformation of ikaite to calcite, and the crystallization of Mg-calcite indicate changing geochemical conditions within a cold vent environment at different times. Ideal conditions for the ikaite formation are given during the establishment of a cold vent site when upward-migrating, methane-rich fluids enhance the anaerobe decomposition of organic matter, which again increases the phosphate and alkalinity concentrations near the sediment surface. Lower rates of organic matter decomposition during on-going venting decrease these high phosphate but also sulphate concentrations and allows other carbonate phases as Mg-calcite to form. This additional carbonate precipitation and the ikaite formation itself lower the high alkalinity and destabilize ikaite, which pseudomorphs to porous calcite. Triggered by the further upward-shifting SO_4/H_2S boundary and increasing methane oxidation rates, the typical cold vent methane-derived carbonate genesis takes place, which cements the sediment pore space and

* Corresponding author. Tel.: +49-431-600-2122; Fax: +49-431-600-2911.
E-mail address: jgreinert@geomar.de (J. Greinert).

0025-3227/03/$ – see front matter
doi:10.1016/S0025-3227(03)00354-2

induces the secondary Mg-calcite crystallization within the glendonite fabric. Taking this scenario into account, ikaite formation should be a common process in the beginning of methane-dominated vent activity at cold bottom water temperatures; glendonite pseudomorphs can be assumed to represent a typical manifestation at fossil and recent cold vents at high latitudes.

Keywords: glendonite; ikaite; C and O isotopes; oxygen isotope fractionation of ikaite; methane venting; Sea of Okhotsk

1. Introduction

Methane-derived carbonates and glendonite aggregates were recovered from an area of active methane venting at the slope of the Sakhalin Peninsula, Sea of Okhotsk. The question arose whether the observed methane-dominated cold venting might also influence the genesis of the pseudomorph phase glendonite and its assumed precursor ikaite. The authigenic formation of carbonates at cold vents, where methane escapes from the seafloor, is a very common process. Independent of the special geological setting of the cold vent system (e.g. at subduction zones or mud mounds), the carbonate precipitation is typically linked to anaerobe methane oxidation and coupled sulphate reduction by archaea and bacteria, which release HS^- and HCO_3^-, the latter of which triggers and enhances the carbonate formation (Iversen and Jørgensen, 1985; Han and Suess, 1989; Thiel et al., 1999; Boetius et al., 2000). Depending on the particular geochemical conditions, authigenic calcite, Mg-calcite, aragonite, proto-dolomite and even dolomite precipitate in different geochemical zones at the sediment surface or in the sediment column (e.g. Burton, 1993; Greinert et al., 2001). In addition to petrographic analyses, carbon and oxygen isotope analyses are commonly used to determine the carbon source and growth temperature. This interpretation helps to identify the diagenetic zone from which the carbonates originate and the mechanisms of their formation.

Natural occurrences of ikaite, the hexahydrate of $CaCO_3$, are less often reported (e.g. Suess et al., 1982; Schubert et al., 1997; Jansen et al., 1987; Whiticar and Suess, 1998; Buchardt et al., 2001). Ikaite constitutes a metastable phase at normal pressure conditions (e.g. Bischoff et al., 1993), but can form under special geochemical conditions if low temperatures are present. If the temperature increases to 5–10°C (Larsen, 1994) or if the geochemical environment changes, ikaite often transforms into calcite. At slow changing rates, calcite pseudomorphs the ikaite without destroying the habitus of the former ikaite, although its volume decreases to 68.6% (Larsen, 1994). Ikaite has been suggested by Shearman and Smith (1985), Shearman et al. (1989) or Larsen (1994) as the precursor of the calcite pseudomorph glendonite (synonyms: *gennoishi*, *thinolite*, *pseudogaylusseite*, *jarrowite*) and Swainson and Hammond (2001) provided additional strong evidence. Nevertheless, a direct relationship has never been proven, but if the suggestion is correct, ikaite has been a common mineral in cold-water environments throughout the geological record as glendonites are known from deposits of Carboniferous to Recent age from high latitudes of the northern and southern hemispheres (e.g. Boggs, 1972; Kaplan, 1979; Kemper and Schmitz, 1981; DeLurio and Frakes, 1999). In the northwestern Pacific region, glendonites have been found offshore Sakhalin, Kamchatka and Hokkaido within Paleogene to Neogene marine deposits (Pleshakov, 1937; Zakharova, 1974; Brodskaya and Rengarten, 1975; Kraevaya et al., 1987) and in Quaternary marine sediments in the Sea of Okhotsk (Astakhov, 1986; Derkachev et al., 2002).

Recent ikaite occurrences in the marine environment are typically linked to low temperatures (< 6°C; see review in Buchardt et al., 2001). Normal seawater is not supersaturated with respect to ikaite at these low temperatures; an additional carbonate increase as well as chemical inhibitors that prevent the growth of anhydrous carbonate phases are essential for the ikaite formation (Bis-

choff et al., 1993; Buchardt et al., 2001). In marine environments the mixing of bicarbonate- and carbonate-rich fluids with Ca-rich interstitial or sea water is probably the most common ikaite forming process. The expulsion of alkaline spring waters into seawater (Ikka Fjord; Buchardt et al., 1997, 2001) and the alkalinity increase due to decomposing organic matter (Bransfield Strait; Suess et al., 1982) have already been reported. Cold fluid venting of reduced geochemical species coupled with the anaerobic oxidation of methane via sulphate reduction constitues another mechanism that might be involved in the ikaite formation as shown here.

Bischoff et al. (1993) calculated a ten-fold increase in alkalinity, or the addition of about 1625 mg HCO_3^- to each litre of seawater, to reach ikaite saturation. To accomplish this, the crystallization of calcite or aragonite must be inhibited by geochemical compounds, e.g. sulphate or phosphate (Mucci, 1986; Burton, 1993). Sulphate is known to slow down the process of calcite/Mg-calcite precipitation and leads to aragonite-rich carbonates in sulphate-enriched environments at cold vents (Savard et al., 1996, Greinert et al., 2001). With respect to ikaite, sulphate is only effective at concentrations in excess of the $CaCO_3$ species in solution (Bischoff et al., 1993). Phosphate plays an important role in the ikaite formation and stability (Buchardt et al., 2001) as it inhibits the calcite and aragonite formation even in trace concentrations (e.g. Burton, 1993). Bischoff et al. (1993) showed that 100 μmol KH_2PO_4 in solution stabilizes ikaite indefinitely and concluded that phosphate is the primary natural control over the persistence of ikaite.

In nature, organic-rich sediments are thought to provide ideal conditions for ikaite formation near the sediment–water interface because of the release of phosphate during organic matter decomposition (Suess et al., 1982; Bischoff et al., 1993; Larsen, 1994). However, the presence of dissolved sulphate greatly decreases the inhibitory effect of phosphate on both calcite and aragonite (Burton, 1993) and thus may also influence the crystallization and stability of ikaite.

2. Study area and sampling procedure

Our studies in the Sea of Okhotsk were carried out within the joint German–Russian project KOMEX. The investigations included direct seafloor observations, coring, trawling, and hydro casts (Fig. 1; Biebow and Hütten, 1999; Biebow et al., 2000) as well as a broad spectrum of geochemical and mineralogical analyses. Two distinctive features characterize the Sea of Okhotsk, the second largest marginal sea of the Pacific Ocean. Firstly, it has a very high primary production with seasonal variations dominated by siliceous plankton (Koblenz-Mischke, 1977). Secondly, it is largely ice-covered from December to April each year and was completely ice-covered during glacial periods.

The high primary production and solid matter discharge of the Amur River causes high concentrations of organic carbon in the sediment. Oil and gas deposits in the shelf region are fuelled by this carbon and are used as an energy source (Kovalchuk et al., 1981; Kharakhinov, 2002). The generation of methane is so immense that methane ebullitions from the seafloor are known from many sites along the entire eastern Sakhalin slope (Ginsburg and Soloviev, 1994; Obzhirov et al., 1999). Escaping gas bubbles form clouds or streams which can be observed as flare-like backscatter signals during single beam echosounder investigations. Some of these flares have been known as very persistent features for more than 20 years indicating a rather constant venting activity (Obzhirov, 1993; Obzhirov et al., 1989, 1999).

The ice coverage in winter causes a strong stratification of the water column. Between 50 and 100 m water depth, the temperature is 0 to −1°C for the whole year. Above, the temperature varies and the surface temperature reaches 14–16°C in the summer months. Below 100 m, the temperature steadily increases and reaches approximately 1°C at 400 m water depth in the summer. The temperature changes seasonally and varies from −1 to 1°C in correlation with down-welling processes of cold surface water that also transports isotopically light water from river runoffs to the seafloor. Seasonal variations of −0.8 to −0.2‰ $\delta^{18}O$

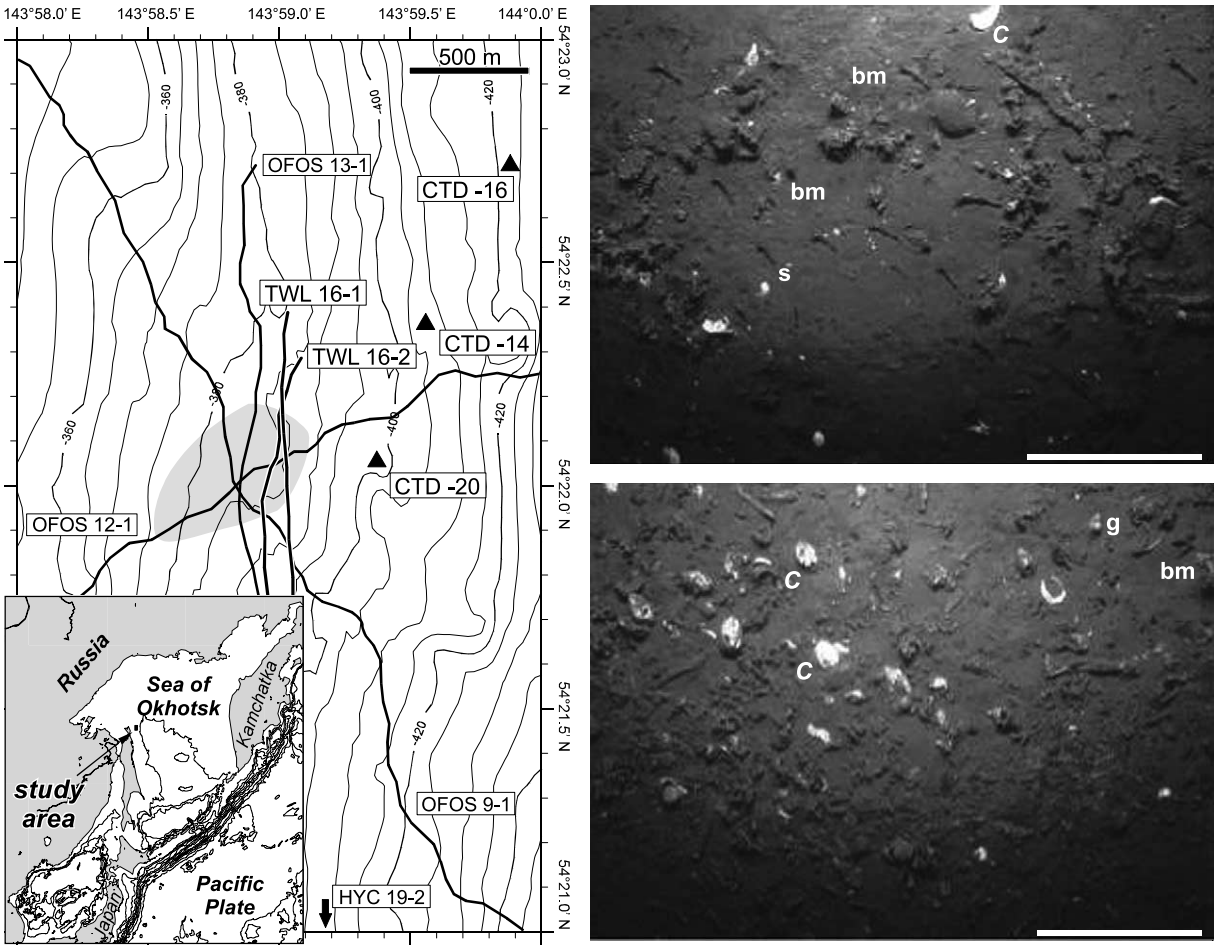

Fig. 1. Map of the Sakhalin study area at the northernmost tip of the Sakhalin Peninsula, Sea of Okhotsk. The gray field marks the area where chemoautotrophic clams, which indicate active fluid venting, were observed during OFOS tracks. The right images show the seafloor with whitish bacterial mats (bm), *Calyptogena* (*C*), gastropods (g) and shrimps (s). Elongated, curved and irregular forms are carbonates, mainly cemented bioturbation traces, which were recovered by trawling (TWL 16-1 and 16-2). Scale bars represent 50 cm. This figure can be downloaded in color at http://www.geomar.de/sci_dptm/publications/.

Standard Mean Ocean Water (SMOW) of the bottom water were observed at a monitoring station during the KOMEX project (1998–1999) in a water depth of 400 m (pers. commun. G. Winckler, 2002).

The carbonates described here were recovered from one of the permanently active flare-areas at the NW end of Sakhalin Island. The seafloor of the area studied was investigated in three TV-observation tracks (OFOS) that showed living chemoautotrophic clams and clam shells of *Calyptogena* (Sahling et al., accepted) as typical visual signs of active fluid venting at depths between 370 and 390 m (Fig. 1). Consecutively, the gently eastward-facing slope was cored for sediment and pore water sampling (HYC 16-2) to study the fluid composition. Trawls (TWL 16-1 and 16-2) retrieved chemoautotrophic fauna and also sampled different kinds of carbonates. Water samples for methane analyses were taken (CTD-14, -16, -20) at the vent site and in the vicinity to explore the impact of methane released into the water column. To ascertain the composition of pore water not influenced by methane vents, a

reference core was taken 6.5 km south of the venting site (HYC 19-2).

The results of these investigations yielded clear evidence of active venting of methane-rich fluids, the authigenic formation of carbonates (presented here), and the occurrence of gas hydrate in the vicinity (Ginsburg and Soloviev, 1994; Soloviev et al., 1994; Biebow and Hütten, 1999; Biebow et al., 2000). Our visual observations showed that methane-derived authigenic carbonates and glendonites only occur in the venting region. Because of this circumstance, the question arises whether the formation of ikaite is favored in areas of methane-dominated cold vents and whether changing geochemical conditions due to varying venting intensity can cause the transformation from ikaite to glendonite. To strengthen our isotopic data base, an ikaite crystal was analyzed, which was sampled in 5.3 m sediment depth 75 km east of the study area in 1996 (SLR 3-3: 54°24.60′N, 145°07.60′E; 1480 m water depth; Nürnberg et al., 1997). The crystal was immediately stored in a deep freezer after recovery and still exists at GEOMAR.

3. Analytical methods

Carbonates were investigated using light microscopy and x-ray diffraction (XRD) for analyzing their mineral composition. For XRD, powdered sub-samples were mixed with corundum as an internal standard to correct 2θ values and estimate the $MgCO_3$ content of the calcitic carbonate phase by the *d*-value of the (104) reflection (Goldsmith et al., 1961). Observations by scanning electron microscopy (SEM) and energy disperse spectroscopy analyses (EDS) provided additional information about the crystal morphology and carbonate chemistry, respectively.

Isotope sub-samples were extracted by a microdrill from the carbonates. Ikaite sub-sampling was undertaken in a freezing room at −23°C. Two sets of sub-samples were analyzed from the ikait crystal. One set was stored at room temperature (~20°C) after sub-sampling and isotopically analyzed approximately two months later. The other set of sub-samples was freeze-dried at −56°C and analyzed some days after drying. Carbon and oxygen isotope measurements were carried out with a 'Finnigan' MAT 252 connected to a Carbo–Kiel online device following the method described by Wachter and Hayes (1985). Replicate analyses of a laboratory standard yielded standard deviations better than 0.03‰ for $\delta^{18}O$ and 0.02‰ for $\delta^{13}C$. All C and O isotopic data for the carbonates shown here are given relative to PeeDee Belemnite (PDB) standard.

To calculate the $\delta^{18}O$ value of the equilibrium source water (δ_{water} vs. SMOW) or to estimate the formation temperature by analyzing $\delta^{18}O$ values of the calcite phases ($\delta_{calcite}$ vs. PDB) we used the equation given by Hays and Grossmann (1991) that was also used by DeLurio and Frakes (1999) for their paleoenvironmental calculations on glendonites:

$$t(^{\circ}C) = 15.7 - 4.36(\delta_{calcite} - \delta_{water}) + 0.12(\delta_{calcite} - \delta_{water})^2$$

To correct the ^{18}O-enrichment due to the Mg-incorporation in Mg-calcite, we subtracted 0.06‰ per each mol% $MgCO_3$ in the calcite lattice (Tarutani et al., 1969).

Methane from water samples was extracted by a vacuum degassing system and analyzed onboard. Pore water of sediment cores was squeezed in a cold room during the cruise; phosphate and alkalinity were measured by photometry and titration; sulphate and organic carbon concentrations were measured onshore by ion chromatography and TCN analyses, respectively.

4. Results

4.1. Petrographic description

The carbonate samples recovered at Station TWL 16-1 and 16-2 can be divided into four groups: (A) Elongated to tube-like forms of cemented sediment (mudstones) with a smooth surface, representing cemented bioturbation traces; (B) roundish forms with smooth surfaces which originate from the cementation of mud pebbles (mudstones); (C) tube-like to irregularly elon-

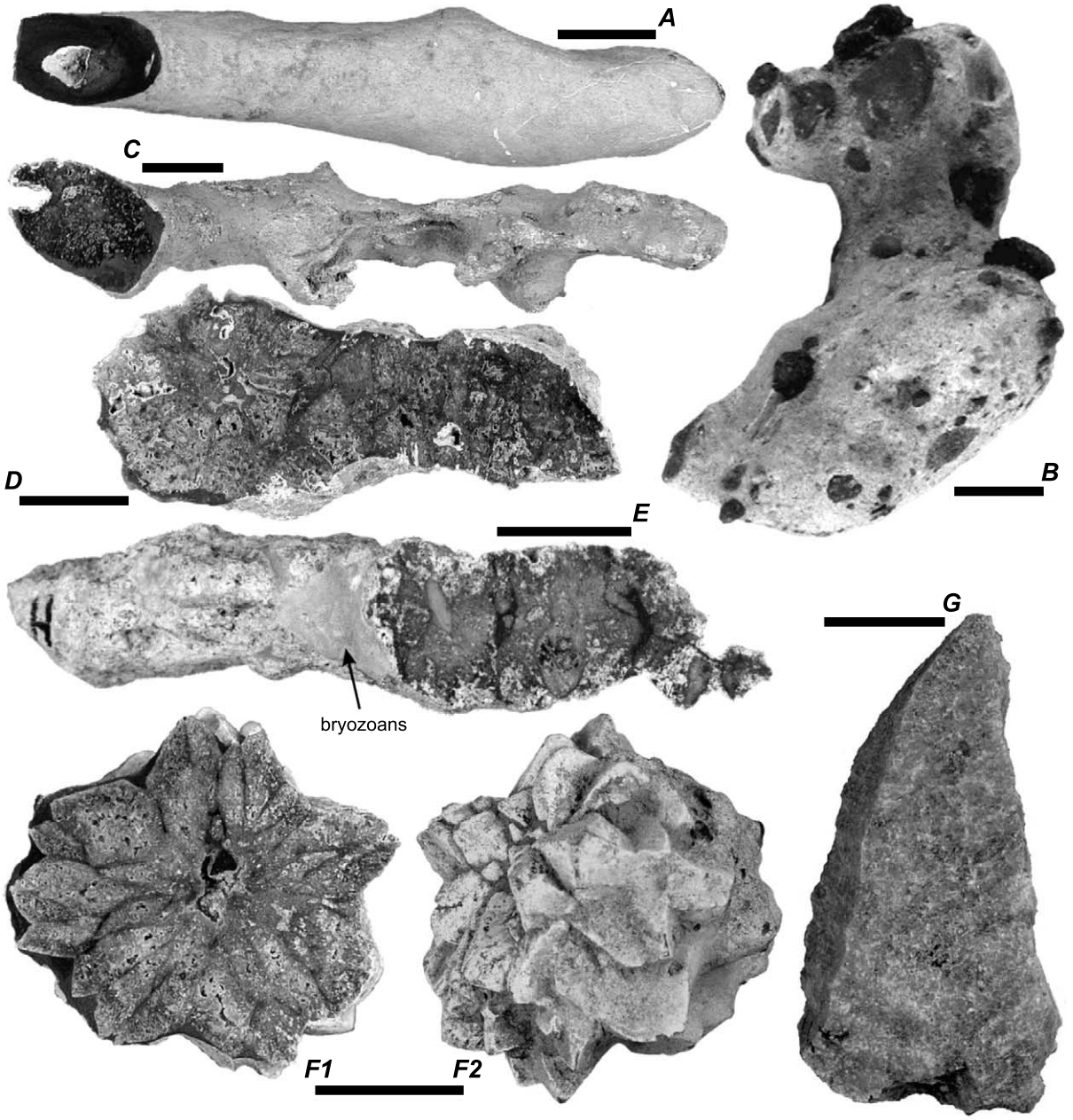

Fig. 2. Carbonate samples from station TWL 16-1 and 16-2. Group A carbonates typically show elongated forms that represent cemented bioturbation traces which sometimes exhibit a central hole with a concentric zonation of the dark sediment matrix (A). They also show transitions to the more roundish forms of cemented mud pebbles of group B (not shown here) with incorporated dropstones (B). Samples of group C are elongated with irregular shapes and rougher, porous surfaces. In cross-section they show a porous cementation of amber-colored carbonate (C–E) and also exhibit remnants of glendonite aggregates (left side in D). The amount of the amber carbonate varies between 10% and 90% and represents pseudomorph calcite after ikaite. Glendonites of group D show typical square-based bi-pyramidal crystals forming a radial aggregate (F1), which model their surface (F2). (G) shows an ikaite crystal of sigmoidal square–prismatic shape, sampled in the Sea of Okhotsk that was isotopically analyzed. All scale bars represent 2 cm length. This figure can be downloaded in color at http://www.geomar.de/sci_dpmt/publications/.

gated forms with uneven and porous surfaces, composed of porous amber-colored carbonate (sparite) and varying amounts of cemented sediment (mudstone); (D) glendonites showing defined, square-based pyramid faces or porous remnants of them at the surface, in cross-section they reveal a porous, amber-colored carbonate cementation (sparite) equivalent to group C concretions; only small amounts of cemented sediment (mudstone) cover glendonite aggregates at their surface (Fig. 2). Because of the petrographic and isotopic similarity between the amber-colored carbonate of group C and D (as will be shown later), we suggest that group C carbonates also represent a former ikaite phase that crystallized in bioturbation traces and later pseudomorphs to calcite. Specimens of all types show patches of white or red bryozoans that cover the surface (Fig. 2D), indicating a seafloor surface exposure for a relatively long period of time.

Elongated specimens of group A have a length of up to 30 cm, diameters of 2–3 cm and a smooth surface. The round to oval-shaped cross-sections often exhibit a central hole several mm to 1 cm in diameter, which forms a tube through the entire specimen. In places, the fine-grained, generally homogeneous sediment matrix shows a concentric zonation around these holes which varies in color between dark gray and lighter gray–brown (Fig. 2A). These zones are separated by thin black lines (<1 mm), which also occur as veins in random distribution. Some elongated samples that are cemented onto each other in a criss-cross orientation also contain dark dropstones of mm to cm in size. The dropstones demonstrate the presence of ice-rafted material in the investigated area (Fig. 2B). Because of their shape, group A samples are interpreted as cemented bioturbation traces. Cementation either occurred in the sediment that filled burrows/trails or in the sediment around them. The latter seems the case with tube-like specimens, which might be used as a pathway for ascending fluid. A formation of the central hole due to fluid or gas migration and a chimney-like genesis as described by Jørgensen (1992) seems rather unlikely.

Roundish forms of group B also have a smooth surface and show the same dark sediment as the elongated specimens. Both sediment-dominated groups A and B are mudstones petrographically, but the group B carbonates represent cemented mud pebbles. Those, too, were recovered in the study area in soft to rigid stages indicating different cementations. In contrast to the dark, inner sediment areas, the surfaces of all recovered group A and B mudstones are light gray to light brown in color. The thickness of this outer rim varies between less than 1 mm and 4 mm, and thicker portions tend to show more brownish colors. This lighter rim is caused by the oxidation of organic matter and pyrite, the latter of which is responsible for the light brown colors.

The more irregular, elongated samples of group C never show a central hole (Fig. 2C). In cross-section an amber-colored, granular and porous cementation becomes visible, which causes a rough and porous appearance on the specimen's surfaces (Fig. 2C,E). Nevertheless, well defined bi-pyramidal forms of cm size are also visible, and a few samples even exhibit aggregates of radially arranged bi-pyramidal forms similar to glendonite (Fig. 2D). Cemented dark sediment occurs as veins (Fig. 2E) or as angular shapes surrounding pyramidal forms or filling the areas between them (Fig. 2D). The amount of sediment varies from 10% to almost 90% in some samples. Because of their size and shape samples of group C are also suggested to represent fillings of bioturbation traces.

The group D glendonites show pyramidal forms at their surfaces (Fig. 2F1) and radially arranged bi-pyramidal crystals of 3 by 1 cm in size in cross-section (Fig. 2F2). Their amber color and porous fabric with pore volumes between nearly 0% and 40% is equivalent to group C carbonates. In contrast to them, the amount of sediment between the bi-pyramidal crystals is much less or does not exist, which indicates a displacive growth in the sediment or at the seafloor surface. Typically, the glendonites are partly covered by a thin sediment coating that smoothes the pyramidal habit on their surface (Fig. 2F1,F2).

In thin section the dark sediment, regardless of the groups discussed above, shows a micritic carbonate cementation of fine sand- to clay-size terrigenous sediment particles (quartz, plagioclase,

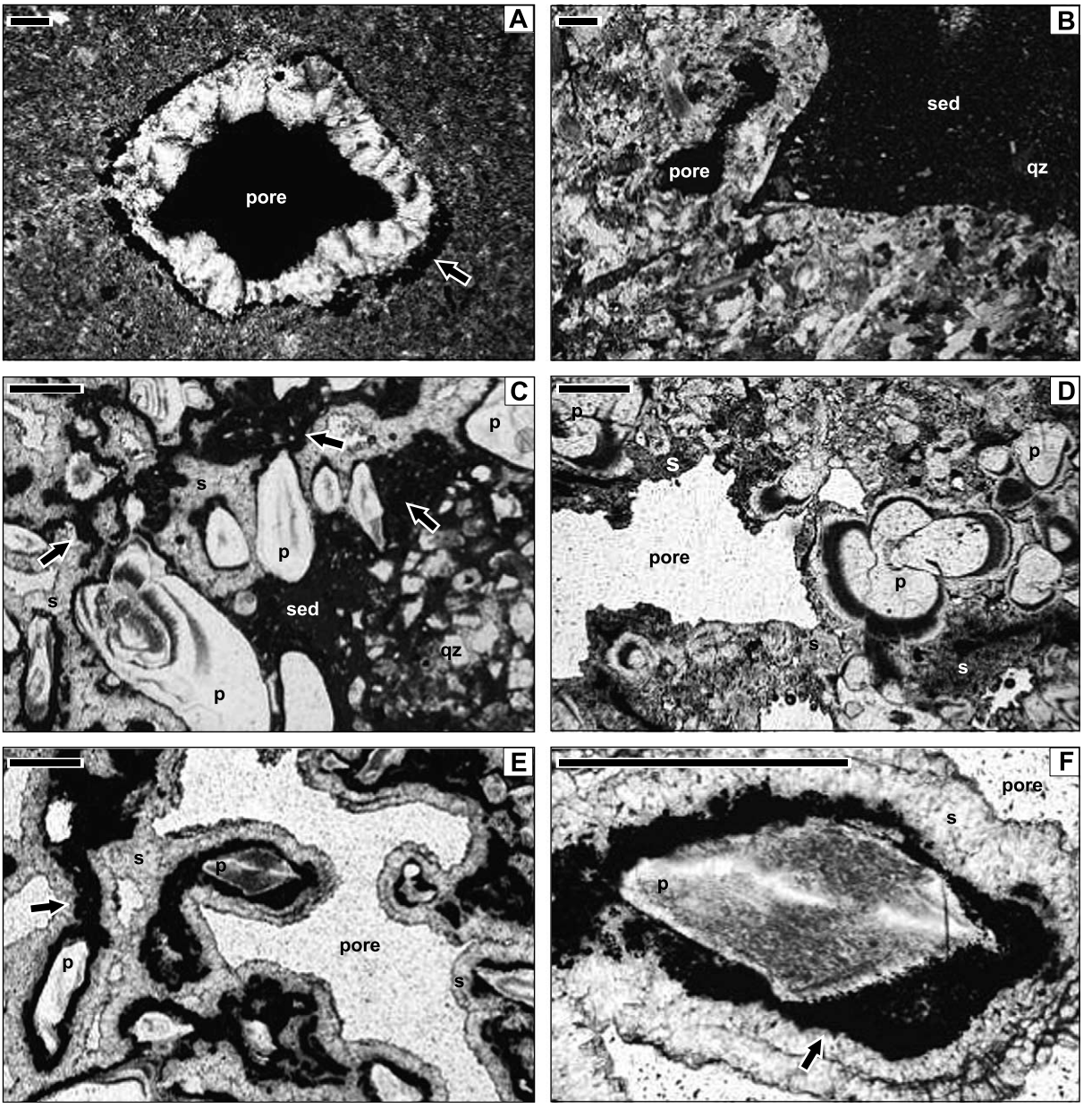

Fig. 3. Thin sections of carbonate samples. (A) Open pore in a silt- to clay-size sediment matrix of a tube-like carbonate sample with pyrite (arrow) and euhedral calcite rim cementation (crossed nicols). (B) Edge of a glendonite sample with randomly oriented calcite crystals and dark sediment (sed) with quartz grains (qz) that often coats glendonite aggregates (crossed nicols). (C) Primary calcite crystals (p) transformed from ikaite are overgrown by pyrite (arrows) and the secondarily formed euhedral MgC (s); dark sediment (sed) with angular quartz grains is visible on the right side (parallel nicols). (D) Glendonite sample with typical, layered impurities in the primary pseudomorph calcite phase (p; also in C) and later rim cements of euhedral MgC (s); pyrite is rare in glendonite samples. (E) Porous area of an amber-colored concretion with a bi-pyramidal pseudomorph calcite crystal rimmed by pyrite and secondary MgC. (F) Close-up of the bi-pyramidal calcite crystal of image E. Scale bars represent 100 μm (A,B) and 500 μm (C–F). This figure can be downloaded in color at http://www.geomar.de/sci_dpmt/publications/.

K-feldspar, kaolinite, muscovite), diatoms and radiolaria (Fig. 3A,B). Feldspar and quartz crystals often occur as larger, angular components, arranged in clusters (Fig. 3A–C) or layers, the latter causing the macroscopically visible zonation in some samples of groups A and B (Fig. 2A). Thin dark lines reveal a greater amount of pyrite either as idiomorphic crystals or with framboidal habitus. Cubic pyrite crystals (5–10 μm) also occur scattered randomly throughout the entire matrix.

Microsparitic to sparititic rim cements of euhedral Mg-calcite are typically found at the edge of the central hole in elongated carbonates of group A. In some of these tubes as well as in smaller pores a rim of idiomorphic pyrite crystals (up to 50 μm thick) is sandwiched between the euhedral rim cement and the sediment (Fig. 3A).

Equivalent pyrite rims are very common in the amber-colored carbonate phase of group C carbonates but seldom occur in glendonites. The internal fabric of group C and D carbonates generally shows a comb-like structure with up to 50% pore volume. Two different carbonate generations are obvious, of which the first one (p in Fig. 3C–F) is composed of oval (Fig. 3C) and sometimes bi-pyramidally-shaped grains (Fig. 3E,F) of up to 1.5 mm in size. They typically show concentric brown impurities of varying thickness (10–100 μm), which become thicker towards the crystal edges and may indicate growth/recrystallization steps (Fig. 3C,D). In group C concretions, the subsequent crystallization of idiomorphic pyrite forms an up to 100 μm-thick layer that occurs as nearly uninterrupted overgrowth in places (Fig. 3E). The second carbonate crystallization (s in Fig. 3C–F) constitutes euhedral calcite of mainly sparitic size. It forms a more or less continuous cement which overlies the primary carbonate grains or the pyrite layer but does not fill the porous fabric entirely (Fig. 3C–E). EDS investigations of glendonites and the amber-colored concretions reveal a significant Mg-enrichment in the secondarily formed carbonate phase, whereas the primary phase contains Ca exclusively.

XRD measurements indicate Mg-calcite (MgC) as the only cementing carbonate phase of the sediment. Measurements of (104) *d*-values result in 6–10 mol% $MgCO_3$ in the Mg-calcite lattice. Analyses of the amber carbonate of both glendonites and carbonates of group C show pure stoichometric calcite or a mixture of calcite and varying amounts of MgC with 6–10 mol% $CaCO_3$ as well. Estimates of the MgC content in those samples were calculated via the area ratio of the (104) reflections and result in up to 60% MgC.

Because of the great similarity in color, the porous and granular fabric of the amber-colored calcite/MgC mixture, and the pyramidal forms observed in group C and D samples, we strongly suggest an original affinity of both groups. Although detailed crystallographic investigations as described by Swainson and Hammond (2001)

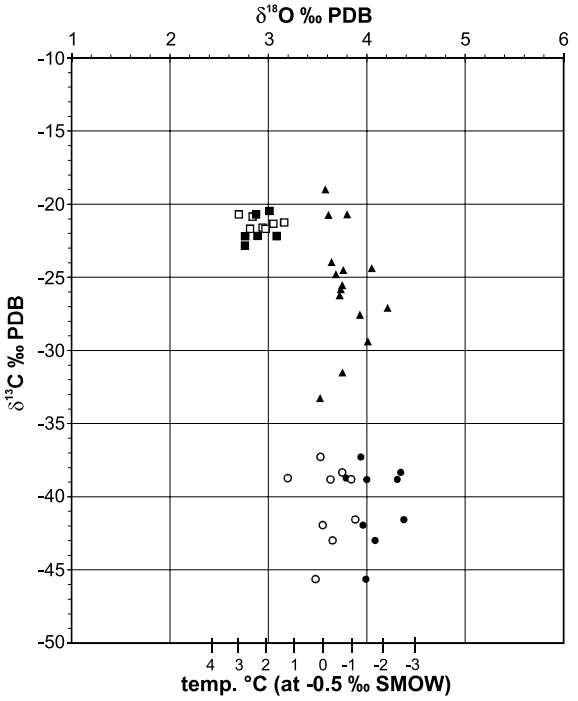

Fig. 4. Carbon and oxygen isotopic data of MgC-cemented sediment (black circles; open circles are values corrected for the $MgCO_3$ content after Tarutani et al., 1969), pseudomorph calcite of glendonite and group C concretions (black triangles) and an ikaite crystal (open squares represent subsamples transformed at 20°C; black squares represent freeze-dried sub-samples). The $\delta^{18}O$-temperature scale at the bottom *x*-axis indicates the temperature for equilibrium crystallization of calcite in water with −0.5‰ SMOW for respective $\delta^{18}O$ values (calculated after DeLurio and Frakes, 1999).

could not be performed to prove that the shown aggregates are really glendonites, their great similarity to specimens described by Larsen (1994), DeLurio and Frakes (1999), Swainson and Hammond (2001) and to calcite aggregates shown by Jansen et al. (1987) convinced us that the shown pseudomorphs are glendonites with ikaite as a precursor for both group D and C carbonates.

4.2. Carbon and oxygen isotope investigations

Analyses for $\delta^{13}C$ and $\delta^{18}O$ were performed on cemented sediment from bioturbation casts (group A), former mud pebbles (group B) and group C concretions. Amber-colored calcite was sub-sampled from glendonites and group C concretions; freeze-dried and at room temperature transformed calcite of the ikaite crystal were analyzed as well (the transformation to calcite was verified by XRD). The analyses were preformed to determine the possible carbon source and to estimate the water temperature of the source water during the carbonate formation.

The MgC phase of cemented sediment shows $\delta^{13}C$ values between -38 and $-46‰$ and varies from 3.2 to 4.4‰ in $\delta^{18}O$ (Fig. 4). With a range from -19 to $-34‰$, the carbon isotope values of calcite from glendonite pseudomorphs and group C concretions are significantly higher. Their oxygen isotope values are similar to MgC cemented sediments, but with a smaller range from 3.5 to 4.2‰.

Isotope analyses of the ikaite crystal from Station SLR 3-3 show lower $\delta^{18}O$ values of 2.7–3.2‰ independently of whether the sub-samples transformed at room temperature or were freeze-dried. With a range from -22.8 to $-20.5‰$, the $\delta^{13}C$ values of the ikaite represent the ^{13}C-enriched data analyzed for pseudomorph calcite. Sub-samples dried at room temperature were taken from different points at one crystal face of the ikaite, but oxygen and carbon isotope data do not show any trends related to their position.

4.3. Geochemical water column and pore water analyses

To characterize the geochemical environment of the vent area and to investigate whether fluid venting has recently been active, samples from the water column and pore water squeezed from sediment cores were analyzed both onboard and in onshore labs. During two CTD hydrocasts (CTD 16 and 20; Fig. 1) we detected extreme methane anomalies at approximately 80 m above the seafloor. The maximum concentrations reached 9000 nl/L at station CTD 20 and 4500 nl/L at CTD 16, but generally the methane concentrations were significantly elevated (>1000 nl/L) at both stations below 170 m water depth. CTD 14, sampled one year before, did not show such high concentrations but analyses of up to 210 nl/L below 150 m also indicate a methane-enrichment compared to the background concentrations of about 50 nl/L (Biebow and Hütten, 1999; Biebow et al., 2000).

Pore water data of core HYC 16-2 within the active vent zone (based on the occurrence of chemosynthetic species; Sahling et al., accepted) exhibit sulphate, ammonium and alkalinity values typical of active fluid venting and anaerobic methane oxidation. Although the sulphate concentrations decreased dramatically from 25 mM at 15 cm core depth to 4.1 mM at 150 cm, the ammonium concentrations were less than 13 μM throughout the entire core. Alkalinity is inversely correlated to sulphate and increases from 7 meq./l at the top to 32 meq./l at the bottom of the core (Fig. 5).

The increasing phosphate concentrations below

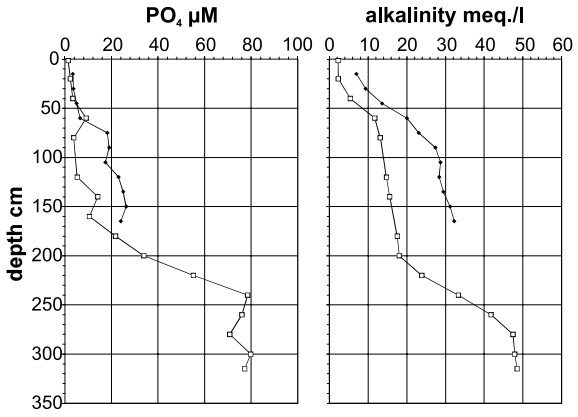

Fig. 5. Pore water data from vent station HYC 16-2 (black diamonds) and the reference site HYC 19-2 (open squares).

1 m core depth reaching 26 µM at 150 cm (HYC 16-2) are important for the formation of ikaite. A much stronger PO_4 increase is documented in the pore water of the 3.2-m-long reference core at station HYC 19-2. Here, the concentrations reach up to 80 µM below 240 cm depth (Fig. 5). Furthermore, an increase in alkalinity can be observed, but the concentrations are lower than those at station HYC 16-2. By contrast, at station HYC 19-2 ammonium shows a steady increase with depth, showing the highest concentration at the core base (2.2 mM). Analyses of the content of organic carbon show high values with a mean of 1.4 wt% for both cores.

5. Discussion

5.1. Recently active venting

The investigation of vent sites raises questions about the recent venting activity, strength, and timing of the onset of the cold vent system. The investigated area at the Sakhalin Shelf had definitely been active during the cruises in 1998 and 1999, as evidenced by the living chemoautotrophic fauna, hydroacoustic flares and geochemical methane anomalies in the water column. The varying methane concentrations in the water column may point to a non-permanent methane expulsion and, but probably more important here, a methane distribution strongly influenced by currents.

The upward migration of methane through the sediment and anaerobic methane oxidation via sulphate reduction is reflected in the sulphate/ammonium correlation at station HYC 16-2. Unchanging ammonium values and decreasing sulphate concentrations at cold vent sites classically point to a biogenic consumption of sulphate due to methane oxidation (e.g. Han and Suess, 1989; Greinert et al., 2002). In contrast, reference core HYC 19-2 shows a sulphate/ammonium correlation that is typical of pore waters influenced by the degradation of organic matter (Fig. 6), which is a common process in the diagenesis of organic-rich sediments such as these occur in the Sea of Okhotsk.

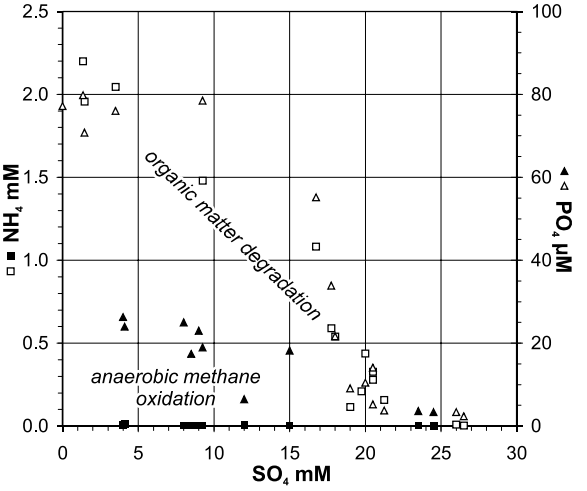

Fig. 6. Correlations between NH_4/PO_4 and SO_4 concentrations imply methane oxidation via sulphate reduction at station HYC 16-2 (black symbols) and anaerobic degradation of organic matter at the reference station HYC 19-2 (open symbols).

5.2. Methane- and organic matter-derived carbonates

Negative $\delta^{13}C$ values of the sediment-cementing MgC phase indicate anaerobically oxidized methane as an important carbon source. Values between −37 and −46‰ constitute the typical range for methane-derived carbonates found in ancient and recent cold vent environments (e.g. summarized by Campbell et al., 2002). Carbon isotope values around −20‰, as measured for the ikaite crystal and the ^{13}C-rich glendonite samples, suggest an incorporation of carbon from organic matter. Both the decomposition of organic matter and the oxidation of methane via sulphate reduction increase the alkalinity and thus force and trigger the carbonate formation (e.g. Paull et al., 1992; Greinert et al., 2001).

Consequently, the varying carbon isotope values of glendonites and pseudomorph calcite (groups C and D) reflect a mixture of methane-derived carbon and carbon from organic matter. Petrographic observations show that MgC overgrows the primary pseudomorph calcite phase. Thus, it is probable that the secondary MgC phase crystallizes from methane in the same manner as the MgC of the cemented sediment and

induces $\delta^{13}C$ values below −20‰, which is the value of MgC-free glendonite samples and the ikaite crystal. Assuming a $\delta^{13}C$ value of −43‰ for the methane-derived MgC phase (the mean of exclusively MgC-cemented sediment samples; Fig. 4) and −20‰ for the ikaite-derived calcite, an amount of up to 60% MgC can be estimated to have precipitated in the porous fabrics of the glendonites and amber-colored concretions. This estimate fits in with the calculated MgC/calcite ratio of our XRD analyses and the theoretical decrease in volume during the transformation of ikaite to calcite (Shearman and Smith, 1985). Thus the varying $\delta^{13}C$ values of the glendonites investigated here can simply be explained by a mixture of two carbonate phases which crystallized during different times and from different C-sources. The primary calcite phase preserves the organic matter-derived carbon of its precursor ikaite, the secondary MgC phase incorporates methane–carbon during its sediment cementation and crystallization in the porous glendonite/amber calcite concretion fabric.

5.3. $\delta^{18}O$ temperature signatures

Temperature calculations using the oxygen isotope composition of a carbonate phase must be applied with caution. Even if the source water is known isotopically, one still has to assume equilibrium crystallization with the source water. Because of the morphologically well-defined glendonite pseudomorphs, a slow transformation from ikaite to calcite is suggested (Larsen, 1994). Assuming that the transformation of ikaite to calcite and the later genesis of the MgC phase all occurred in equilibrium with the pore water, the ^{18}O values of both pseudomorph calcite and MgC (MgC values corrected for their $MgCO_3$ content; Fig. 4) can be used to calculate the ancient bottom water temperature. Using a $\delta^{18}O$ source water value of −0.5‰ SMOW as found for the present bottom water (pers. commun. G. Winckler, 2002), the ancient bottom water temperature can be predicted to have ranged between −2 and 1°C (Fig. 4). This temperature range fits in with the seasonal temperature changes of −1 to 1°C in the study area (Biebow et al., 2000). The $\delta^{18}O$ values of the ikaite crystal indicate slightly higher temperatures ranging from 1.5 to 3°C at −0.5‰ SMOW (Fig. 4). This discrepancy can be explained by the higher bottom water temperature of 2°C at the sampling depth of 1480 m.

Moreover, our data allow speculations about the primary isotopic signal of the ikaite, the ^{18}O fractionation during its formation and the possible isotope fractionation during the transformation to calcite. Indicated by equivalent $\delta^{18}O$ values of ikaite samples that transformed at 20°C and those which could not equilibrate with the crystal water due to the freeze-drying process, no equilibration between CO_3^{2-} and the crystal water seems to occur during the ikaite–calcite transformation. Thus the measured $\delta^{18}O$ values of pseudomorph calcite presumably represent the original ikaite–water fractionation during the ikaite genesis. At 2°C and −0.5‰ SMOW the ^{18}O-fractionation of ikaite with 3‰ $\delta^{18}O$ (Fig. 4) results in a fractionation factor α of 1.0345 ($\alpha = [1000+\delta^{18}O_{mineral}]/[1000+\delta^{18}O_{water}]$, both δ-values relative to the same standard). In comparison, equilibrium precipitation of calcite at 2°C also results in 3‰ $\delta^{18}O$ (Fig. 4). This supports the assumption that calcite and ikaite are similar in their oxygen isotope fractionation during their formation at low temperatures and thus allows the use of a calcite equilibration formula to calculate the formation temperature of ikaite and its pseudomorph calcite phase.

5.4. Ikaite/glendonite genesis – related to methane venting?

The investigated cold vent area shows geochemical conditions and a methane-derived authigenic carbonate formation typical of many other recent and ancient cold vent sites, too (e.g. Greinert et al., 2001; Aloisi et al., 2002; Michaelis et al., 2002; Campbell et al., 2002). Both the advection of methane and the microbially mediated formation of carbonate via coupled methane oxidation/sulphate reduction processes are shown by our investigations.

Due to the paragenesis of pseudomorphs after ikaite and the methane-derived carbonate precipitation at a cold vent area, we suggest an influence

of the upward-migrating methane-rich fluids on the ikaite origin and the later ikaite–calcite transformation. The methane advection towards shallower sediment depths enhances the anaerobic decomposition of organic matter via sulphate reduction above the SO_4/H_2S boundary. This increases the release of HCO_3^- and PO_4 from organic matter. The upward-migrating fluids push the zone of anaerobic organic matter decomposition towards or even up to the sediment surface, and thus establish the necessary high phosphate and alkalinity concentrations to form ikaite near the sediment surface. As the geochemical environment still contains sulphate, the formation of calcite and MgC is inhibited. Both of these calcite phases, as well as aragonite, are also inhibited by high phosphate concentrations, which allow an extreme increase in alkalinity and provoke ideal conditions for ikaite to form (stage 1 in Fig. 7).

Induced by on-going fluid migration, the SO_4/H_2S boundary moves towards the seafloor surface and caused by the leak of SO_4 and/or decreased amounts of organic matter, the turnover rate of organic matter decomposition and subsequently the phosphate concentration becomes smaller. The crystallization of ikaite itself and the now favored growth of other carbonate phases such as MgC decrease the alkalinity and both low phosphate and lower alkalinity destabilize ikaite and induce the ikaite–calcite transformation (stage 2 in Fig. 7).

Increasing H_2S concentrations, fuelled by deeper sediment horizons and high sulphate reduction rates at the beginning of the microbially mediated methane oxidation via sulphate reduction, allow the formation of pyrite at the SO_4/H_2S boundary. The higher amount of pyrite in the pore space of the amber-colored concretions of group C might be caused by a higher in-situ SO_4-reduction rate and an higher flux of H_2S-rich fluids using the former bioturbation trace and the porous calcite fabric as a preferred pathway (stage 3 in Fig. 7). The oxidation of methane again increases the alkalinity and induces the crystallization of Mg-calcite in the sediment and glendonite pore space, now showing more negative carbon isotopes values typical of methane-derived carbonates at cold vents (stage 4 in Fig. 7). Further studies around cold vents at low bottom water temperatures may show that ikaite is a common precipitation in the vicinity or during the early stage of methane-rich venting.

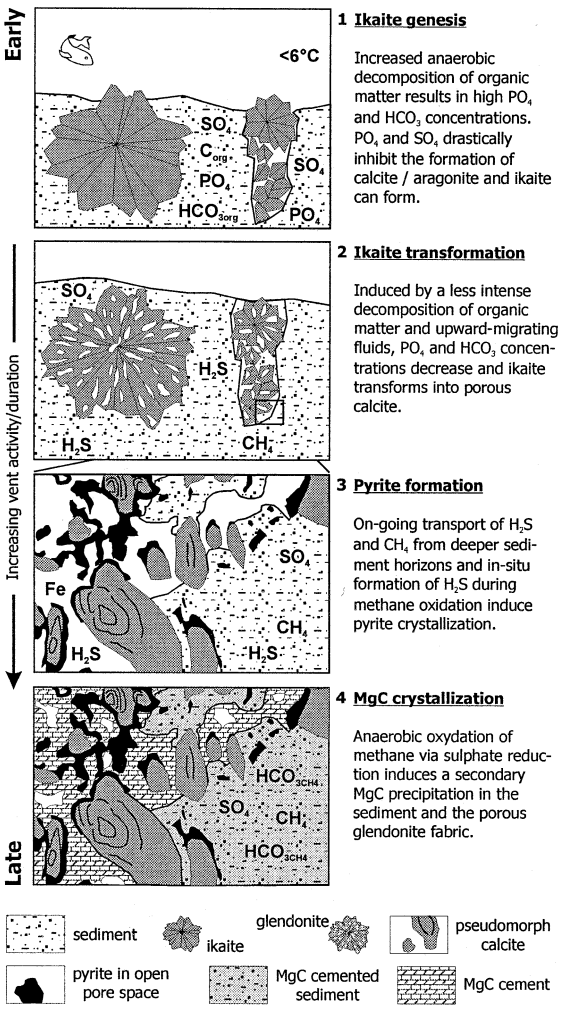

Fig. 7. Scheme of a methane vent-induced ikaite/glendonite formation and secondary methane-derived Mg-calcite crystallization as suggested by glendonite and amber-colored calcite concretions found at a cold vent area at the Sakhalin slope. Stage 3 and 4 are schematic drawings of image C in Fig. 3.

6. Summary and conclusions

Mg-calcite-cemented bioturbation traces and pseudomorph calcite after ikaite (in glendonite shape or as porous, amber-colored calcite concre-

tions) were recovered from an active cold vent area at the shelf of the northernmost tip of Sakhalin, Sea of Okhotsk. Mg-calcite, which exclusively cements the sediment of cemented bioturbation traces, shows negative $\delta^{13}C$ values between -37 and $-46‰$. This is a typical range for carbon derived from the anaerobic oxidation of methane, which induced the Mg-calcite precipitation. Analyses of pseudomorph calcite are less negative (-19 to $-34‰$); the variability can be explained by a mixture of methane- (Mg-calcite) and organic matter-derived carbon (pseudomorph calcite). The two carbonate phases are visible in microscopic investigations and show a primary calcite phase formed from ikaite and a secondary Mg-calcite phase generated from methane within the porous calcite fabric of the former ikaite. The $\delta^{13}C$-enriched end member ($-20‰$) of glendonite samples indicates organic matter as the exclusive carbon source of the former ikaite phase. This isotope value is also in very good agreement with analyses of an ikaite crystal that shows organic matter as carbon source, too ($\delta^{13}C$ -20 to $-22‰$).

That pseudomorph calcite preserves the isotopic signal of the former ikaite can be assumed from freeze-dried and at 20°C transformed ikaite samples, which show identical values in both C and O. Using the mean of the ikaite $\delta^{18}O$ analyzed and a most likely $\delta^{18}O$ value of $-0.5‰$ SMOW for the seawater during the ikaite formation at 2°C, the oxygen isotope fractionation of ikaite can be calculated ($\alpha = 1.0345$), which is equivalent to the calcite fractionation at low temperatures. This supports the use of normal calcite equilibration equations to be applied for paleoenvironmental interpretations from glendonites.

Visual investigations of the seafloor revealed that glendonites/pseudomorph calcite concretions and cemented bioturbation traces occur only in areas of active and ancient fluid venting. This spatial relationship and our petrographic and isotopic investigations sustain the notion that methane-dominated fluid venting influences the ikaite genesis and the ikaite–calcite transformation as well. Due to the increase in anaerobic decomposition of organic matter during the early stages of fluid venting, the geochemical conditions are ideal for the generation of ikaite near the sediment surface (high phosphate concentrations, high alkalinity). On-going fluid venting and the displacement of sulphate and phosphate by upward-migrating fluids from greater depths and the beginning crystallization of other carbonate phases as Mg-calcite may cause the ikaite–calcite transformation. Of course, the occurrence of ikaite and its pseudomorph calcite aggregates are not strictly related to methane-venting, but particularly for fossil occurrences of glendonites cold vents should be taken into account as a possible formation environment.

Acknowledgements

We are indebted to our Russian colleagues and the crews of RV *Lavrentyev* and HS *Gelovany* for their enthusiasm during the cruises, and the technical staff at GEOMAR for fast and professional geochemical and isotopic analyses. Thanks are due also to D. Nürnberg for providing the ikaite crystal and to K. Campbell and B. Buchardt for their very profound and useful reviews. Further, our thanks go to the Federal Ministry of Education and Research for supporting this work through Grant 03G0535A.

References

Aloisi, G., Bouloubassi, I., Heijs, S.K., Pancost, R.D., Pierre, C., Sinninghe Damste, J.S., Gottschal, J.C., Forney, L.J., Rouchy, J.-M., 2002. CH_4-consuming micro-organisms and formation of carbonate crusts at cold seeps. Earth Planet. Sci. Lett. 203, 195–203.

Astakhov, A.S., 1986. Late-Quaternary Sedimentation on the Shelf of the Sea of Okhotsk (in Russian). FESC, AN SSSR, Vladivostok, 140 pp.

Boetius, A., Ravenschlag, K., Schubert, C.J., Rickert, D., Widdel, F., Gieskes, A., Amann, R., Jørgensen, B.B., Witte, U., Pfannkuche, O., 2000. A microbial consortium apparently mediating anaerobic oxidation of methane. Nature 407, 623–626.

Biebow, N., Hütten, E., 1999. Cruise Report: KOMEX I and II (RV Gagarinsky; RV Lavrentyev). GEOMAR Report 82, 270 pp.

Biebow, N., Lüdmann, T., Karp, B., Kulinich, R., 2000. Cruise Report: KOMEX III and IV (RV Gagarinsky; RV Gelovany). GEOMAR Report 88, 296 pp.

Bischoff, J.L., Fitzpatrick, J.A., Rosenbauer, R.J., 1993. The solubility and stabilization of ikaite ($CaCO_3$*$6H_2O$) from 0° to 25°C: Environmental and paleoclimatic implications for thinolite tufa. J. Geol. 101, 21–33.

Boggs, R.S., 1972. Petrography and geochemistry of rhombic calcite pseudomorphoses from mid-Tertiary mudstones of the Pacific, Northeast U.S.A.. Sedimentology 19, 95–99.

Brodskaya, N.G., Rengarten, N.V., 1975. Organogenic nature of diagenetic gennoishi-like formations: The problems of lithology and geochemistry of sedimentary rocks and ores (in Russian). Nauka, 312–323.

Buchardt, B., Seaman, P., Stockmann, G., Vous, M., Wilken, U., Düwel, L., Kristiansen, A., Jenner, C., Whiticar, M.J., Kristensen, R.M., Petersen, G.H., Thorbjørn, L., 1997. Submarine columns of ikaite tufa. Nature 390, 129–130.

Buchardt, B., Israelson, C., Seaman, P., Stockmann, G., 2001. Ikaite tufa in Ikka Fjord, southwest Greenland: Their formation by mixing of seawater and alkaline spring water. J. Sediment. Res. 71, 176–189.

Burton, E.A., 1993. Controls on marine carbonate cement mineralogy: Review and reassessment. Chem. Geol. 105, 163–179.

Campbell, K.A., Farmer, J.D., Des Marais, D., 2002. Ancient hydrocarbon seeps from the Mesozoic convergent margin of California: Carbonate geochemistry, fluids and palaeoenvironments. Geofluids 2, 63–94.

DeLurio, J.L., Frakes, L.A., 1999. Glendonites as a pleoenvironmental tool: Implications for early Cretaceous high latitude climates in Australia. Geochim. Cosmochim. Acta 63, 1039–1048.

Derkachev, A.N., Obzhirov, A.I., Bohrmann, G., Greinert, J., Suess, E., 2002. Authigenic mineral formation at the sites of cold gas–fluid emanations on the bottom of the Sea of Okhotsk. In: Likht, F.R. (Ed.), Conditions of the Generation of Bottom Sediments and Related Mineral Deposits within Marginal Seas (in Russian). Dalnauka, Vladivostok, pp. 47–60.

Ginsburg, G.D., Soloviev, V.A., 1994. Submarine Gas Hydrates (in Russian). VNII Okeangeologiya, St. Petersburg, 199 pp.

Goldsmith, J.R., Graf, D.L., Heard, H.C., 1961. Lattice constants of the calcium–magnesium carbonates. Am. Mineral. 46, 453–457.

Greinert, J., Bohrmann, G., Suess, E., 2001. Methane-venting and gas hydrate-related carbonates at the Hydrate Ridge: Their classification, distribution and origin. In: Paull, C.K., Dillon, W.P. (Eds.), Natural Gas Hydrates: Occurrence, Distribution, and Detection. Geophysical Monograph 124, pp. 99–113.

Greinert, J., Bollwerk, S.M., Derkachev, A., Bohrmann, G., Suess, E., 2002. Massive barite deposits and carbonate mineralization in the Derugin Basin, Sea of Okhotsk: Precipitation process at cold vent sites. Earth Planet. Sci. Lett. 203, 165–180.

Han, M.W., Suess, E., 1989. Subduction-induced pore fluid venting and the formation of authigenic carbonates along the Cascadia continental margin: Implications for the global Ca-cycle. Palaeogeogr. Palaeoclimatol. Palaeoecol. 71, 97–118.

Hays, P.D., Grossmann, E.L., 1991. Oxygen isotopes in meteoric calcite cements as indicators of continental paleoclimate. Geology 19, 441–444.

Iversen, N., Jørgensen, B.B., 1985. Anaerobic methane oxidation rates at the sulphate–methane transition in marine sediments from Kattegat and Skagerrak (Denmark). Limnol. Oceanogr. 30, 944–955.

Jansen, J.H.F., Woensdregt, C.F., Kooistra, M.J., Van der Gaast, S.J., 1987. Ikaite pseudomorphs in the Zaire deep-sea fan: An intermediate between calcite and porous calcite. Geology 15, 245–248.

Jørgensen, N.O., 1992. Methane-derived carbonate cementation of marine sediments from the Kattegatt, Denmark: Geochemical and geological evidence. Mar. Geol. 103, 1–13.

Kaplan, M.E., 1979. Calcite pseudomorphoses (pseudogeilyusite, yarovite, thinolite, glendonite, gennoishi) in sedimentary rocks. The origin of pseudomorphoses (in Russian). Lithol. Miner. Res. 5, 125–141.

Kemper, E., Schmitz, H.H., 1981. Glendonite – Indikatoren des polarmarinen Ablagerungsmilieus. Geol. Rundsch. 70, 759–773.

Kharakhinov, V.V., 2002. Tectonics and oil–gas contents of the Okhotsk Sea region (in Russian). In: Alekseev, M.N. (Ed.), Geology and Mineral Resources of the Russian Shelf Areas. GEOS, Moscow, pp. 106–114.

Koblenz-Mischke, O.J., 1977. Primary Production of the Pacific Ocean (in Russian). Biology of the Pacific Oceans, vol. 1, Nauka, Moscow, pp. 62–65.

Kovalchuk, V.S., Kuklich, L.A., Mishakov, G.S., Tronov, Yu.A., 1981. Predictions of the oil and gas contents for the north-eastern shelf of Sakhalin (in Russian). Geol. Nephti Gasa (Oil and Gas Geol.) 2, 6–12.

Kraevaya, T.C., Chelebaeva, A.I., Shantser, A.E., 1987. The morphological types of gennoishi in Cenozoic deposits of Kamchatka and their possible climate-stratigraphic significance (in Russian). Lithol. Miner. Res. 6, 131–135.

Larsen, D., 1994. Origin and paleoenvironmental significence of calcite pseudomorphs after ikaite in the Oligocene Creed Formation, Colourado. J. Sediment. Res. 64, 593–603.

Michaelis, W., Seifert, R., Nauhaus, K., Treude, T., Thiel, V., Blumenberg, M., Knittel, K., Gieseke, A., Peterknecht, K., Pape, T., Boetius, A., Amann, R., Jorgensen, B.B., Widdel, F., Peckmann, J., Pimenov, N.V., Gulin, M.B., 2002. Microbial reefs in the Black Sea fueled by anaerobic oxdation of methane. Science 297, 1013–1015.

Mucci, A., 1986. Growth kinetics and composition of magnesian calcite overgrowth precipitated from seawater: Quantitative influence of orthophosphate ions. Geochim. Cosmochim. Acta 50, 2255–2265.

Nürnberg, D., Baranov, B., Karp, B., 1997. RV Akademik Lavrentyev Cruise 27. Cruise Report: Gregory. GEOMAR Rep. 60, 143 pp.

Obzhirov, A.I., 1993. Gas Geochemical Fields of the Near-Bottom Layers of Seas and Oceans (in Russian). Nauka, Moscow, 139 pp.

Obzhirov, A.I., Kazanskiy, B.A., Melnichenko, Y.I., 1989. Effect of the sound dispersion within the near-bottom waters of the marginal parts of the Okhotsk Sea (in Russian). Tikhookeanskaya Geol. (Pacif. Geol.) 2, 119–121.

Obzhirov, A.I., Astakhova, N.V., Lipkina, M.I., 1999. Gas-geochemical Zoning and Floor Mineral Associations of the Sea of Okhotsk (in Russian). Dalnauka, Vladivostok, 184 pp.

Paull, C.K., Chanton, J.P., Neumann, A.C., Coston, J.A., Martens, C.S., 1992. Indicators of methane-derived carbonates and chemosynthetic organic carbon deposits: Examples from the Florida Escarpment. Palaios 7, 361–375.

Pleshakov, N.B., 1937. Tertiary Deposits from the Ukhtolokskiy Area, Western Kamchatka (in Russian). Publ. VNIGRI, Ser. A., 123, 92 pp.

Savard, M.M., Beauchamp, B., Veizer, J., 1996. Significance of aragonite cements around Cretaceous marine methane seeps. J. Sediment. Res. 66, 430–438.

Sahling, H., Galkin, S.V., Salyuk, A., Greinert, J., Foerstel, H., Piepenburg, D., Suess, E., accepted. Depth-related structure and ecological significance of cold seep communities – A case study from the Sea of Okhotsk. Deep-Sea Res. I.

Schubert, C.J., Nürnberg, D., Scheele, N., Pauer, F., Kriews, M., 1997. ^{13}C isotope depletion in ikaite crystals: Evidence for methane release from the Siberian shelves? Geo-Mar. Lett. 17, 169–174.

Shearman, D.J., Smith, A.J., 1985. Ikaite, the parent mineral of jarrowite-type pseudomorphs. Proc. Geol. Assoc. Lond. 96, 305–314.

Shearman, D.J., McGugan, A., Stein, C., Smith, A.J., 1989. Ikaite, $CaCO_3{\cdot}6H_2O$, precursor of the thinolites in the Quartenary tufas and tufa mounds of the Lahontan and Mono Lake Basins, western United States. Geol. Soc. Am. Bull. 101, 913–917.

Soloviev, V.A., Ginsburg, G.D., Obzhirov, A.I., Duglas, V.K., 1994. Gas hydrates of the Okhotsk Sea (in Russian). Otechestvennaya Geol. (Native Geol.) 2, 10–17.

Suess, E., Balzer, W., Hesse, K.-F., Müller, P.J., Ungerer, C.A., Wefer, G., 1982. Calcium carbonate hexahydrate from organic-rich sediments of Antarctic Shelf: Precursors of glendonites. Science 216, 1128–1131.

Swainson, I.P., Hammond, R.P., 2001. Ikaite, $CaCO_3 \times 6 H_2O$: Cold comfort for glendonite as palaeothermometers. Am. Mineral. 86, 1530–1533.

Tarutani, T., Clayton, R.N., Mayeda, T.K., 1969. The effect of polymorphism and magnesium substitution on oxygen isotopic fractionation between calcium and water. Geochim. Cosmochim. Acta 33, 987–996.

Thiel, V., Peckmann, J., Seifert, R., Wehrung, P., Reitner, J., Michaelis, W., 1999. Highly isotopically depleted isoprenoids: Molecular markers for ancient methane venting. Geochim. Cosmochim. Acta 63, 3959–3966.

Wachter, E.A., Hayes, J.M., 1985. Exchange of oxygen isotopes in carbon dioxide-phosphoric acid systems. Chem. Geol. 52, 365–374.

Whiticar, M.J., Suess, E., 1998. The cold carbonate connection between Mono Lake, California and the Bransfield Strait, Antarctica. Aquat. Geochem. 4, 429–454.

Zakharova, M.A., 1974. The Lithology of the Sakhalin Paleogene Deposits and the Conditions of their Formations (in Russian). Nauka, Novosibirsk, 107 pp.